International Journal of Engineering & Technology, 7 (4) (2018) 3286-3293

International Journal of Engineering & Technology

Website: www.sciencepubco.com/index.php/IJET
doi: 10.14419/ijet.v7i4.15842
Research paper

Acoustic model of the human outer ear

J. Melloui [1] *, O. Bouattane [1], J. Bakkoury [1]

[1] SSDIA Laboratory, Hassan II University of Casablanca, ENSET of Mohammedia, Mohammedia, Morocco
**Corresponding author E-mail: jihane.melloui@gmail.com*

Abstract

The outer ear is an important part of the human auditory periphery. Its main function is to amplify the incoming sound signal. This amplifi-cation depends on the length and the shape of the ear canal and the concha.
There are various techniques used to model the outer ear, including physical models, finite element models, and electroacoustic models. Current electroacoustic models assume a uniform or gradually varying cross-section in a discontinuous manner of the ear canal.
In this paper, an acoustic model is developed and considers four types of acoustic resonators to take account for the variability of cross sec-tion along the outer ear. Our model is validated against results encountered in the literature. The validated model is used in a parametric study to analyze the effect of the concha and the residual ear modelling on the frequency response of the outer ear

Keywords: *Acoustic Resonator; Concha, Eardrum; Outer Ear Model; Transfer Matrix; Residual Ear.*

1. Introduction

The human auditory periphery consists of three distinct parts: the outer, middle and inner ear that combine to ensure one of the major senses, which is hearing. It converts acoustic pressure signals (i.e.vibrations) into nervous impulses for interpretation by the brain. This mechanism can be thought of as a biological transduction of vibrations to nervous impulses.
The outer ear (Figure 1) consists of a horn (the visible part of the ear) that behaves like an acoustic antenna whose function is to capture the sound waves from the environment and channel them to the eardrum via the concha and the auditory canal [1]. The concha and the ear canal act like acoustic resonators that selectively amplify and transmit to the middle ear, via the eardrum, certain frequencies that depend directly on the length and the shape of the ear canal [2]. The inner section of the auditory canal is shaped up by a boney cavity. The skin of this boney cavity becomes thinner towards the tympanic membrane to help direct the incoming sound with minimal absorption along the auditory canal [3].

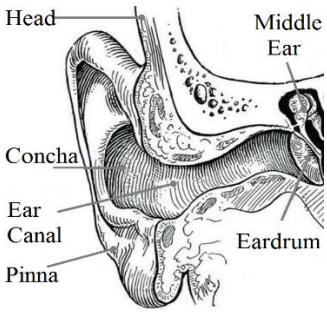


Fig. 1: Anatomy of the Outer Ear [7].

To simulate the functioning of the outer ear, various modelling techniques can be used to approximate the actual behavior of the human auditory system [4]-[6]. The most used techniques include, mathematical, functional, finite element and electro-acoustic modelling techniques.
Mathematical models generally have complex equations and their solutions are often tedious. The complex geometry, ultra-structural characteristics, non-homogenous and anisotropic material properties of biological systems (such as the auditory peripheral system) can be modelled using a finite element model [4].
Functional models offer a way to observe the input-output relationship of a system by not explicitly modelling the internal physical mechanisms of the auditory system. These models often neglect or simplify the outer ear and middle ear models. Although this simplification gives a computationally inexpensive input-output relationship, it restricts the application of the functional auditory model [8].
Electro-acoustic models give a simple and effective way of modelling the functionality of the auditory system based on the close link between acoustic and electrical engineering [8], [9]. Although finite element models give more information than electro-acoustic models [8], acoustical and electrical models generally give a simpler way of analyzing a system and deriving a transfer function. Various hearing conditions (i.e. normal hearing, partial hearing and no hearing) can be simulated by adjusting the parameters modelling the auditory system [10].
The quality of the model essentially depends on two factors, the model's structure which determines its basic capabilities and the proper choice of parameters. Parameter identification such as the external ear shape and pressure wave parameters is therefore as important as the structural design. An accurate, comprehensive model of the human ear can provide better understanding of sound transmission, and can be used for assessing the influence of diseases on hearing and the treatment of hearing loss. The advantages associated with using the acoustical model results in it being the modelling approach of choice for this study.
One of the most used electroacoustic model of the outer ear is developed by Giguere and Woodland [5]. This model included the outer ear diffraction system, the concha and the auditory canal. The concha and auditory canal were modelled as transmission

Copyright © 2018 J. Melloui et. al. This is an open access article distributed under the Creative Commons Attribution License, which permits unrestricted use, distribution, and reproduction in any medium, provided the original work is properly cited.

lines of constant radii [5]. This model was created to give the possibility of dealing with speech and hearing problems.
Thejane [11] studied the influence of the number of segments used in the auditory canal transmission line model of Giguere and Woodland. The shape of the auditory canal is estimated using a pair of second order polynomial function. This function uses radii of the auditory canal published by Gan et al. [4].
Although the study conducted by Zheng et al. [12] proves the suitability of the Giguere and Woodland model, the model has a few deficiencies. As argued by Thejane in [10], the Giguere and Woodland concha and auditory canal models are only valid for frequencies up to 7100 Hz and 8000 Hz, respectively.
Gan et al [4] proposed a finite element model to provide a better understanding of sound transmission and assess the influence of diseases on hearing and hearing loss treatment. They modelled the auditory canal as a tube of irregular shape having three main radii, namely the radius near the tympanic membrane, the radius at the center of the auditory canal and the radius at the entrance of the auditory canal. Although the mesh allows for the shape of the auditory canal to be closely followed, the computation time becomes more expensive.
The electrical model used by Giguere and Woodland [5] incorporates the external ear diffraction system, the concha as well as the auditory canal. However the Gan et al. [4] external ear finite element model falls short in this area since it only incorporates the effect of the auditory canal.
Hiipakka et al. [6] constructed an auditory canal simulator and a dummy head to study the effects of the outer ear on sound pressure at the tympanic membrane with insert-type headphones. The results proved that the length of the auditory canal has an effect on the pressure frequency responses at the auditory canal and at the tympanic membrane.
Volandri et al. [13] modeled the auditory canal and the tympanic membrane using the finite element method to study the distribution of sound pressure and the displacements in the tympanic membrane during propagation of high frequency sounds.
Deng et al. [14] model the ear canal as a multi-sectional acoustic tube with a gradually varying cross-sectional area function and propose a method for deriving the relationship between the ear canal area function and the eardrum reflection coefficient given the acoustic impedance at the entrance of the ear canal.
This shows that electroacoustic auditory canal models available in the literature [5] assume a uniform or gradually varying radius when computing the transmission line model of the auditory canal. Since the actual shape of the auditory canal has a varying radius along its length, a more accurate representation of the auditory canal shape is required.
The objective of this study is to develop a physical model of the outer ear by considering an acoustic model of the concha, the auditory canal and the residual ear (eardrum effect) (Figure 2) by taking into consideration the variability of their sections in order to better approximate the real shape of the outer ear. This acoustic model is based on the method of transfer matrices.
A validation study is conducted by comparing the frequency response obtained using the developed acoustic model against results available in the literature.
The validated model is then used in a parametric analysis to study the effect of concha and eardrum on the frequency response of the outer ear.

2. Methodology of work

2.1. Transfer matrix method

To analyze the propagation of acoustic waves through the outer ear, the transfer matrix method is used. Each part of the outer ear (concha, auditory canal and eardrum) will be modelled using one or more cascaded acoustic resonators (Figure 2). Since we are studying acoustic resonators with 'n' elements, the method of the transfer matrix is more adapted in comparison with the analytical method to study acoustic properties such as resonant frequencies, phase angles. Each resonator can be simply considered as a black box with input and output ports.

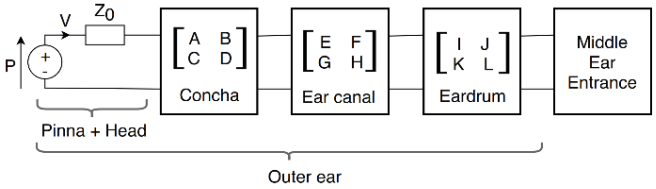


Fig. 2: Acoustic Model of the Outer Ear.

By adopting the sound pressure p(x) and the mass velocity v(x) as the two state variables, the following matrix relation (Figure 3) can be written in order to link the variables of state of both sides of the subscribed acoustic resonator element 'n'.

$$\begin{bmatrix} p_{n-1} \\ v_{n-1} \end{bmatrix} = \begin{bmatrix} \text{Transfer matrix for} \\ \text{n-th element} \end{bmatrix} \begin{bmatrix} p_n \\ v_n \end{bmatrix}$$

Fig. 3: Transfer Matrix of the N-TH Element.

Where p_n and v_n are the acoustic pressures and the mass velocity at the input of the n-th resonator and p_{n-1} and v_{n-1} are the acoustic pressures and the mass velocity at the output of the (n-1)-th resonator.
The equivalent transfer matrix of each outer part is obtained by multiplying in turn the individual transfer matrices of each resonator by the connection matrices if needed. Using the same technic, the transfer matrix for the whole outer ear can be easily obtained using the boundary condition of the n-th output port $v_n = 0$ which represents the infinite impedance of the tympanic membrane (Figure 4).

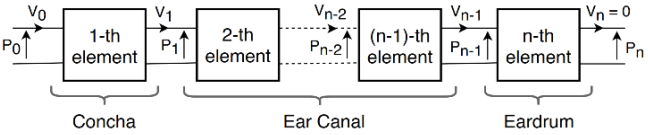


Fig. 4: Element Definition of Each Part of the Outer Ear Acoustic Resonator and Boundary Conditions.

This method will allow us to study the frequency response of the ear canal and analyze the effect of concha and residual ear on resonant frequencies obtained from the acoustic model. A comparison in terms of resonant frequencies obtained from the hereby developed model against results encountered in the literature will permit to validate our model. Several studies have shown that the outer ear resonates for a frequency between 2700 Hz and 5000 Hz [15].

2.2. Sound field

In order to write the individual transfer matrix that represents an acoustic resonator element, we rely on the Webster horn [16] equation (Equ.1). This equation is used to describe the pressure wave in a slowly varying cross section duct.

$$\frac{\partial^2 p(x,t)}{\partial t^2} - c^2 \frac{\partial^2 p(x,t)}{\partial x^2} - \frac{c^2}{S(x)} \frac{dS(x)}{dx} \frac{\partial p(x,t)}{\partial x} = 0 \quad (1)$$

Where: t is time in s, x is one-axis dimension in m, S(x) is the canal section in m², c is air speed in m/s.
In writing $p(x,t) = p(x)e^{j2\pi ft}$, one can get to the wave equation (2) that does not admit a general solution. It can however be solved for some specific forms [17], [18]. In this study, this equation will be solved for canals with uniform, conical and hyperbolic sections varying along its length.

$$\frac{\partial^2 p(x)}{\partial^2 x}+\frac{1}{S(x)}\frac{dS(x)}{dx}\frac{dp(x)}{dx}+K^2\,p(x)=0 \tag{2}$$

With K is the wave number in rad/m in the n-th segment which can be defined in equation (3) as in [19].

$$K=\frac{2\pi f}{c}-\frac{2j}{D_m c}\sqrt{\pi f \upsilon} \tag{3}$$

Where f is frequency of the sound in Hz, D_m is the mean diameter of the canal in m, υ is kinematic viscosity coefficient of the air in m²/s.
For human ear modeling, it is recommended by Hudde [9] to replace the wave number defined in equation (3) by the wave number that takes into account the attenuation of sound in the human ear described in equation (4).

$$K=\frac{2\pi f}{c}-\frac{0.0582\,j}{D_m c}\sqrt{f} \tag{4}$$

Once the expression of sound pressure p(x) known, one can easily determine the mass velocity v(x) since the two entities are linked by the dynamic equilibrium equation [17] defined by the equation (5).

$$\frac{1}{S}\frac{\partial v}{\partial t}+\frac{\partial p}{\partial x}=0 \tag{5}$$

3. Acoustic resonators

To study the pressure wave propagation from the concha entrance to the eardrum through the ear canal, four types of acoustic resonators with varying cross-sectional area are considered (Figure 5). Each n-th segment of a part of the outer ear will be modeled using one type of acoustic resonator segments (i.e uniform, stepped, conical and hyperbolic) which come closest to its real shape. Acoustic resonators of length ln are considered to have a circular periphery with a section S_n of a radius r_n.

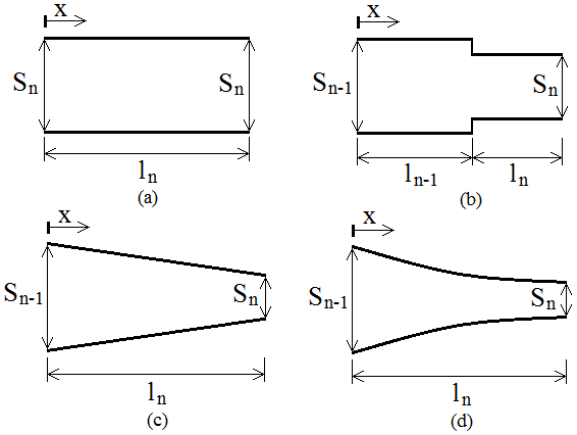


Fig. 5: Section Variation of the N-TH Element of the Resonator A) Uniform B) Stepped C) Conical D) Hyperbolic.

Section variation function of the uniform (U), stepped (S), conical (C) and hyperbolic (H) acoustic resonator segments (U) are defined in equations (6), (7), (8) and (9) respectively.

$$S_U(x)=\pi r_n^2 \tag{6}$$

$$S_S(x)=\begin{cases}\pi r_{n-1}^2 & if \quad x<l_{n-1}\\ \pi r_n^2 & if \quad x\geq l_{n-1}\end{cases} \tag{7}$$

$$S_C(x)=\pi(r_{n-1}+\gamma x)^2$$

Where

$$\gamma=\frac{r_n-r_{n-1}}{r_{n-1}\,l_n} \tag{8}$$

$$S_H(x)=\pi r_{n-1}^2 e^{\frac{2x}{l_n}\ln\left(\frac{r_n}{r_{n-1}}\right)} \tag{9}$$

3.1. Uniform acoustic resonator

The differential equation of pressure variation (Equation 10) is obtained by replacing the section function in equation (2).

$$\frac{\partial^2 p(x)}{\partial^2 x}+K^2 p(x)=0 \tag{10}$$

Solving the differential equation (10) leads to the pressure variation along the uniform acoustic resonator (Equ. 11). The mass velocity (Equ. 12) can then be deducted using equation (5).

$$p(x)=A_1\cos(K x)+A_2\sin(K x) \tag{11}$$

$$v(x)=\frac{-j\,S_U(x)}{c}\left(A_2\cos(K x)-A_1\sin(K x)\right) \tag{12}$$

Where A_1 and A_2 are integration constants.
Boundary conditions (Figure 4) are used in equations (11) and (12) to obtain the system of equations (13).

$$p_{n-1}=A_1\ ;\ p_n=A_1\cos(K l_n)+A_2\sin(K l_n)\ ;$$

$$v_{n-1}=\frac{-j\,S_{n-1}}{c}A_2\ ;\quad v_n=\frac{-j\,S_n}{c}\left(A_2\cos(K l_n)-A_1\sin(K l_n)\right) \tag{13}$$

After some rearranging of the equation (13), the transfer matrix of the uniform acoustic resonator can be obtained (Equation 14)

$$M_{U,n}=\begin{bmatrix}A_U & B_U\\ C_U & D_U\end{bmatrix}$$

Where:

$$A_U=D_U=\cos(K l_n)\ ;$$

$$B_U=-j\frac{c}{S_n}\sin(K l_n)\ ;$$

$$C_U=-j\frac{S_n}{c}\sin(K l_n) \tag{14}$$

Transfer matrix elements A_U and D_U are numbers, B_U has a unit of an impedance, and C_U has a unit of an admittance.

3.2. Stepped acoustic resonator

In the case where two uniform resonators are successive, it is necessary to add a connection matrix (Equ. 15) to take into account the sudden change of the section along its length. The assembly of these resonators is called hereby a stepped acoustic resonator.

$$M_{UC,\,n-1,\,n}=\begin{bmatrix}1 & 0\\ 0 & \frac{S_{n-1}}{S_n}\end{bmatrix} \tag{15}$$

The transfer matrix for stepped acoustic resonator is defined in equation (16).

$$M_{S,n}=M_{U,\,n-1}\times M_{UC,\,n-1,\,n}\times M_{U,\,n} \tag{16}$$

3.3. Conical acoustic resonator

The wave pressure and the mass velocity in the conical acoustic resonator are described respectively by the equations (17) and (18).

$$p(x)=x'(A_1e^{-jKx}+A_2e^{jKx}) \tag{17}$$

$$v(x)=\frac{-j\,S_C(x)\;x'}{Kc}\left[(\gamma x'+jK)A_1e^{-jKx}+(\gamma x'-jK)A_2e^{jKx}\right] \tag{18}$$

Where

$$x'=\frac{1}{1+\gamma x} \tag{19}$$

The transfer matrix for conical acoustic resonator is defined in equation (20).

$$M_{C,n}=\frac{1}{1+\gamma l_n}\begin{bmatrix}A_C & B_C\\ C_C & D_C\end{bmatrix}$$

Where

$$A_C=\cos(Kl_n)+\frac{\gamma\sin(Kl_n)}{K}\;;$$

$$B_C=-j\frac{c}{S_{n-1}}\sin(Kl_n)\;;$$

$$C_C=\frac{-j\,S_n}{cK}\left[\frac{-\gamma^2 l_n}{1+\gamma l_n}\cos(Kl_n)+\left(K+\frac{\gamma^2}{(1+\gamma l_n)K}\right)\sin(Kl_n)\right]\;;$$

$$D_C=\frac{S_n}{S_{n-1}}\left(\cos(Kl_n)-\frac{\gamma}{(1+\gamma l_n)K}\sin(Kl_n)\right) \tag{20}$$

One can easily check that if S_{n-1} is equal to S_n, the matrix transfer of conical resonator is equal to the one of uniform acoustic resonator.

3.4. Hyperbolic acoustic resonator

The wave pressure and the mass velocity in the hyperbolic acoustic resonator are described respectively by the equations (21) and (22).

$$p(x)=A_1e^{-iK_hx}+A_2e^{+iK_hx} \tag{21}$$

$$v(x)=\frac{S_H(x)}{cK}\left[A_1(K_h-j\delta)e^{-jK_hx}+A_2(K_h+j\delta)e^{+jK_hx}\right] \tag{22}$$

Where:

$$K_h=\sqrt{K^2-\frac{1}{l_n^2}\left(\ln\left(r_n/r_{n-1}\right)\right)^2} \tag{23}$$

$$\delta=\frac{1}{l_n}\ln\left(\frac{r_n}{r_{n-1}}\right) \tag{24}$$

After some calculations, the transfer matrix obtained for hyperbolic acoustic resonator is defined using equation (25).

$$M_{H,n}=\begin{bmatrix}A_H & B_H\\ C_H & D_H\end{bmatrix}$$

Where:

$$A_H=e^{\delta l_n}\left(\cos(K_h l_n)-\frac{\delta}{K_h}\sin(K_h l_n)\right);$$

$$B_H=-j\,e^{-\delta l_n}\frac{c}{S_{n-1}}\frac{K}{K_h}\sin(K_h l_n)\;;$$

$$C_H=-j\,e^{-\delta l_n}\frac{S_n}{c}\frac{K}{K_h}\sin(K_h l_n)\;;$$

$$D_H=e^{-\delta l_n}\left(\cos(K_h l_n)+\frac{\delta}{K_h}\sin(K_h l_n)\right) \tag{25}$$

4. Outer ear modelling

4.1. External ear

The model parameters of the external ear used (P and Z_0) are defined as the Thevenin equivalent circuit parameters (Figure 2) of the Bauer's external ear model [20]. Bauer's model assumes that the principal obstacle (upper torso and head) confronting the incident free-field sound wave P_i can be represented by a sphere with effective radius r_S. The ear opening is represented by an orifice with a radius r_{CH} which corresponds to the effective radial size of the concha at the base of the pinna.

$$P=\frac{1+2j\frac{\pi r_s f}{c}}{1+j\frac{\pi r_s f}{c}}\,P_i \tag{26}$$

$$Z_0=\frac{\frac{\rho c}{\pi r_{ch}^2}\left(1+\frac{r_{ch}}{1.4r_s}\right)+j\,\frac{\rho f}{r_s}\left(1+\frac{r_s^2}{r_{ch}^2}\right)}{\left(1-j\frac{c}{1.4\pi f r_{ch}}\right)\left(1+j\frac{\pi f r_{ch}^2}{c r_s}\right)} \tag{27}$$

Where ρ is the air density in kg/m^3

4.2. Concha

Given the actual shape of the concha, this outer ear part can be modeled using a single-element acoustic resonator that takes into account its hyperbolic or conical shape (The resonator type that is the closest to the actual shape will be considered).

4.3. Ear canal

In order to approximate the real form of the auditory canal, four types of acoustic resonator have been considered: uniform, stepped, conical and hyperbolical section variation. The auditory canal will be modeled as cascaded acoustic resonators of same or

different types. The section variation function obtained from the equivalent resonator needs to have a correlation coefficient R that is minimum of 97% with the real section variation of the ear canal. This determines the number of segments of acoustic resonator to use to model with good precision the ear canal.

4.4. Eardrum

The effect of an eardrum on sound transmission in the ear canal is modeled as an effective impedance concentrated at the center (umbo) of the eardrum as in [9, 21 22]. The umbo point is at a distance about 4 mm from the end of the ear canal for average ears.

Several studies [5], [6], [10], [21] modeled the eardrum effect as an obstacle in the umbo point which corresponds to an infinite impedance. Deng et al. [14], modeled the residual ear canal (from the umbo to the eardrum) using a four-sectional tube with same length with stepped cross-sectional area.

In this study, we will model the residual ear canal using either stepped or conical acoustic resonator.

4.5. Flow diagram

The general flow diagram followed in this study in explained in Figure 6. The actual dimensions (lengths and sections) of the outer ear are taken as the starting point. The boundaries of each part of the outer ear (concha, ear canal, residual ear) must be defined. Thereafter, the modeling of each part of the outer ear using acoustic resonator elements can be done.

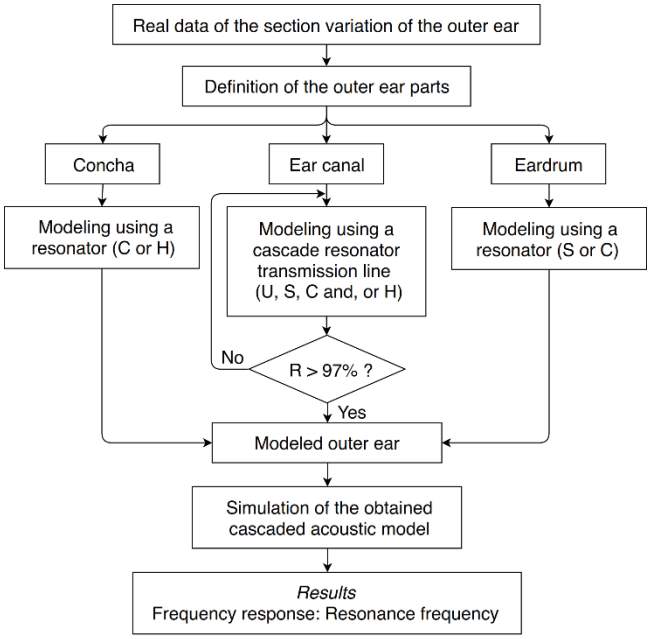


Fig. 6: General Flow Diagram.

5. Validation study

For the purpose of validation, the acoustic behavior in terms of resonant frequencies obtained from the hereby proposed acoustic model is compared to those encountered in the literature. To permit the comparison, dimension data of outer ear published by Volandri [13], Thejane [11] and Stinson [21] are considered.

Volandri [13] modeled the outer ear using FEM method to conduct a harmonic analysis. At first, he modeled a human auditory canal by a uniform tube, and in a second time, he modeled the outer ear consisting of a concha, an auditory canal and a tympanic membrane using a pseudo-anatomical geometry (shape approximating the actual shape of the outer ear). Resonators types and their diameter and length dimensions used in the acoustic model for the uniform tube and the pseudo-anatomic geometry are presented in Figure 7 and figure 8 respectively.

Thejane [11] applied an electroacoustic model on an ear canal that consists in four cascaded segments each one with a distinct diameter retrieved by a radius-length relationship function for the auditory canal. Diameter and length dimensions used in the acoustic model for Thejane's ear canal are shown in Figure 9.

Stinson [21] used a mathematical model on 15 human ear canals. Area-functions used to predict the sound-pressure-distribution along the human ear canal are obtained experimentally. In the original work, each ear canal is referred by "Canal i" or "C_i" (i ranging from 1 to 15), the same notation will be kept in the present study. In the validation study, only canal 4 is treated, the resonators used and their dimensions are presented in Figure 10.

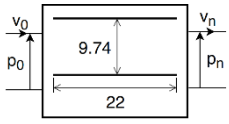


Fig. 7: Acoustic Model of Volandri's Uniform Shaped Ear Canal.

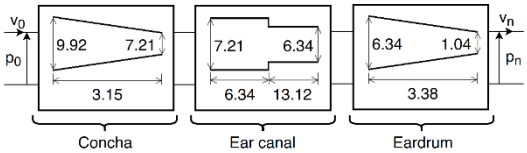


Fig. 8: Acoustic Model of Volandri's Anatomic Shaped Outer Ear.

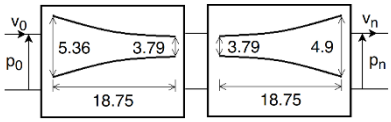


Fig. 9: Acoustic Model of Thejane's Ear Canal.

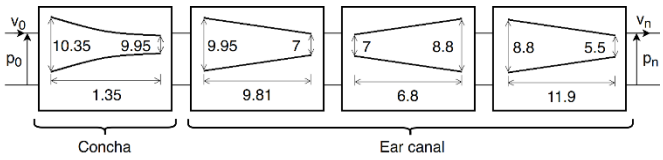


Fig. 10: Acoustic Model of Stinson's Ear Canal with Concha (Canal 4).

As it can be seen from table 1, the error between the results encountered in the literature concerning the three first resonance frequencies (1-Ref, 2-Ref and 3-Ref) and those obtained by the proposed acoustic model (1-AR, 2-AR and 3-AR) remains acceptable.

Table 1: Prediction of the First Three Resonant Frequencies

Resonance frequency (Hz)	Volandri[13] Uniform	Volandri[13] Anatomic	Thejane [11]	Stinson[21] Canal 4
1 - Ref	3864	3961	2692	3297
1 - AR	3863	4007	2301	3427
Error	-0,03%	1,16%	-14,5%	3,94%
2- Ref	11601	11103	7079	10478
2- AR	11590	11010	6905	10510
Error	-0,09%	-0,84%	-2,46%	0,31%
3- Ref	19367	17119	10878	15319
3- AR	19320	18350	11370	15770
Error	-0,24%	7,19%	4,52%	2,94%

6. Parametric analysis

In order to study the effect of the concha and the eardrum impedance on the frequency response of the outer ear, a test matrix of 18 cases (left and right ear, with and without concha, with and without taking account for the eardrum effect) involving 6 outer ears (C2, C4, C6, C9, C13 and C15) is developed.

Measurements of real outer ears published by Stinson et al. [21] are used to calculate the section variation function that will be used hereby to deduce the optimal number of acoustic resonator segments (Figure 11 and 12).

The dimensions in terms of diameter D_n and length l_n of the obtained acoustic resonator are presented in table 2 and table 3. This acoustic resonator model the concha (CON), the ear canal compounded of n segments (EC-n) and the residual ear (ED). Only the uniform, conical and hyperbolic types are considered in this modeling seeing that they are more representative or the actual shape of the outer ear.

Since the human auditory area covers three decades of frequency (from 20 Hz to 20 kHz), the frequency domain used in this study will be of the same range.

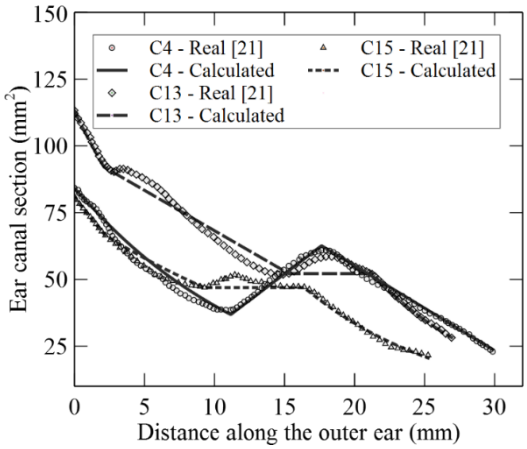


Fig. 11: Approximation of the Shape of the Left Outer Ears.

Table 2: Parameters of Acoustic Resonator of the Left Outer Ears

		Acoustic resonator segment dimensions (mm)							
		Uniform		Conical			Hyperbolic		
		D_n	l_n	D_{n-1}	D_n	l_n	D_{n-1}	D_n	l_n
C4	CON	-	-	-	-	-	10.35	9.95	1.35
	EC-1	-	-	9.95	7	9.81	-	-	-
	EC-2	-	-	7	8.8	6.8	-	-	-
	EC-3	-	-	8.8	5.5	11.9	-	-	-
	ED	-	-	5.5	0.1	2.98	-	-	-
C13	CON	-	-	12.01	10.83	2.3	-	-	-
	EC-1	-	-	10.83	8.15	13	-	-	-
	EC-2	8.15	5.58	-	-	-	-	-	-
	EC-3	-	-	8.15	6	5.65	-	-	-
	ED	-	-	6	0.1	2.65	-	-	-
C15	CON	-	-	-	-	-	10.15	9.08	2.2
	EC-1	-	-	9.08	7.73	6.73	-	-	-
	EC-2	7.73	7.12	-	-	-	-	-	-
	EC-3	-	-	7.73	5.12	9.36	-	-	-
	ED	-	-	5.12	0.1	2.54	-	-	-

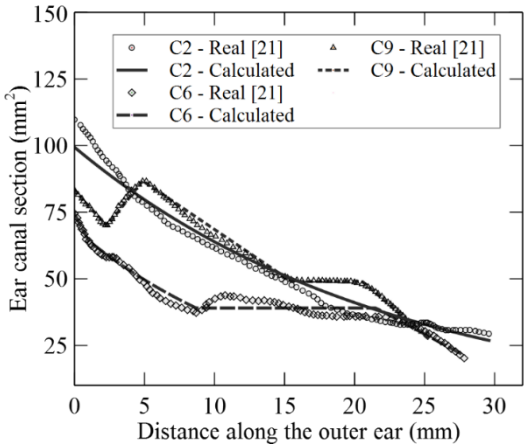


Fig. 12: Approximation of the Shape of the Right Outer Ears.

Table 3: Parameters of Acoustic Resonator of the Right Outer Ears

		Acoustic resonator segment dimensions (mm)							
		Uniform		Conical			Hyperbolic		
		D_n	l_n	D_{n-1}	D_n	l_n	D_{n-1}	D_n	l_n
C6	CON	-	-	-	-	-	9.74	9.04	1.04
	EC-1	-	-	9.04	7.13	7.67	-	-	-
	EC-2	7.13	15.15	-	-	-	-	-	-
C2	EC-3	-	-	7.13	5.3	3.87	-	-	-
	ED	-	-	5.3	0.1	2.77	-	-	-
	CON	-	-	-	-	-	11.76	10.7	3
	EC-1	-	-	10.7	6.35	20.1	-	-	-
	EC-2	6.35	6.65	-	-	-	-	-	-
	ED	-	-	6.35	0.1	2.97	-	-	-
C9	CON	-	-	-	-	-	10.3	9.44	2.35
	EC-1	-	-	9.44	10.5	2.53	-	-	-
	EC-2	-	-	-	-	-	10.5	8.04	10.2
	EC-3	8.04	5.14	-	-	-	-	-	-
	EC-4	-	-	8.04	5.8	4.74	-	-	-
	ED	-	-	5.8	0.1	2.49	-	-	-

7. Results and discussion

7.1. Frequency response of ear canal

The sound pressure transfer function (SPTF) of the studied cases is calculated using equation (28). The results are shown in Figures 13 and 14 for the left and right outer ears, respectively.

$$SPTF = 20 \log \left| \frac{p_n}{p_0} \right| \tag{28}$$

According to Figure 13 and 14, one can observe that the first resonant frequency occurred at 4016, 3317, 3503, 4526, 4182 and 4316 Hz for respectively the canal 2, 4, 6, 9, 13 and 15. The second resonant frequency ranged from 9592 Hz for canal 2 to 11807 Hz for canal 15. The third resonant frequency ranged from 14941 Hz for canal 4 to 19340 Hz for canal 9.

The height of the peaks of sound pressure gain is of the order of 25-32 dB at the studied frequency domain.

These values will be used as a reference to study the effect of the concha and the eardrum impedance on the frequency response of the outer ear.

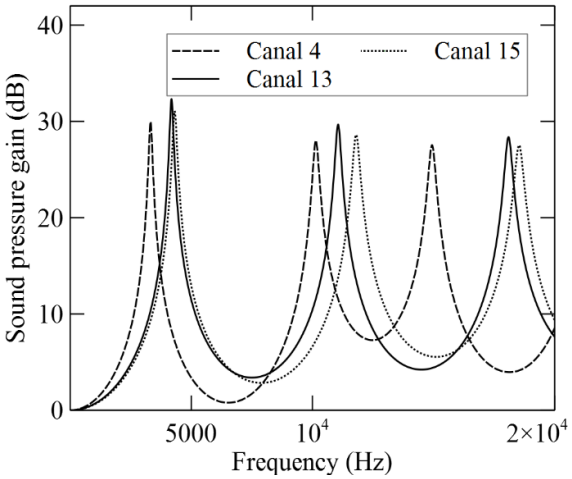


Fig. 13: SPTF of the Left Ear Canals.

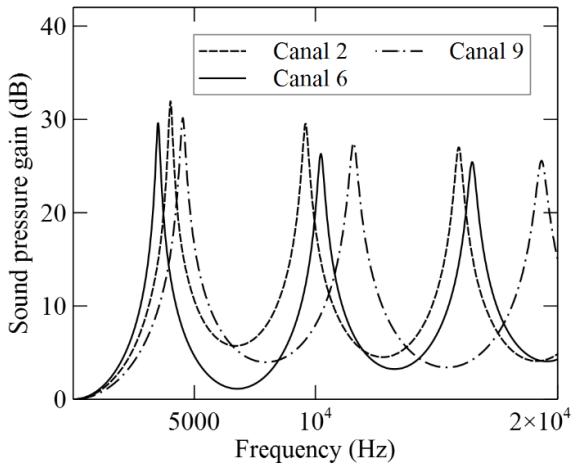


Fig. 14: SPTF of the Right Ear Canals.

7.2. Frequency response of ear canal with concha

If we consider the first resonant frequencies obtained from the simulation of the left and right outer ears (Figure 15 and 16) and comparing them to those obtained from the simulation that ignores the effect of the concha (Figure 13 and 14), it is found that the resonant frequency increases by 8.2, 3.3, 2.6, 5.3, 7.3 and 7.8% for the Canal 2, 4, 6, 9, 13 and 15, respectively when this effect is taken into consideration.

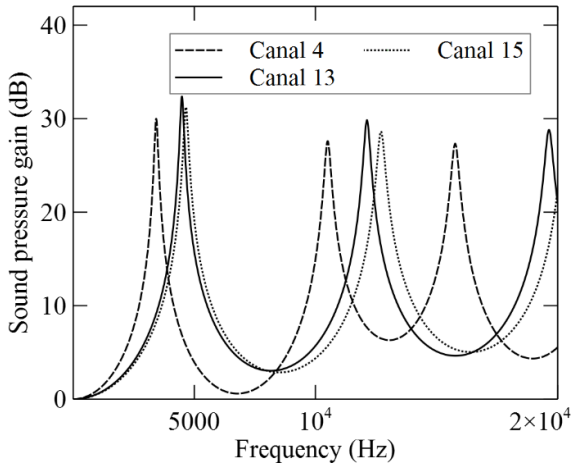


Fig. 15: SPTF of the Left Ear Canals with Concha.

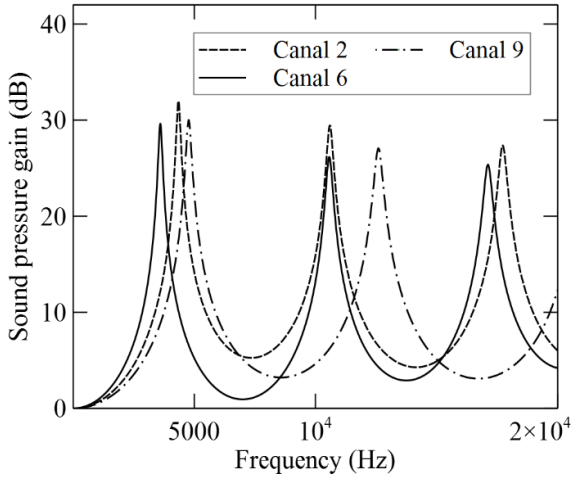


Fig. 16: SPTF of the Right Ear Canals with Concha.

7.3. Frequency response of outer ear

In previous simulation, the residual ear was modelled using an obstacle in the umbo location, in the present simulation, the residual ear is modelled as an acoustic resonator with a form and dimensions that approximate its real shape. This modelling has an effect on the value of the eardrum impedance (Figure 17 and Figure 18).

The induced effect is a decrease in the value of the resonance frequency ranging from 2% observed for channel 4 to 4.5% observed for channel 9 in comparison with the cases of Figure 14 and Figure 15. A decrease is also observed in the order of 1 to 2% of the sound pressure gain in the studied frequency interval.

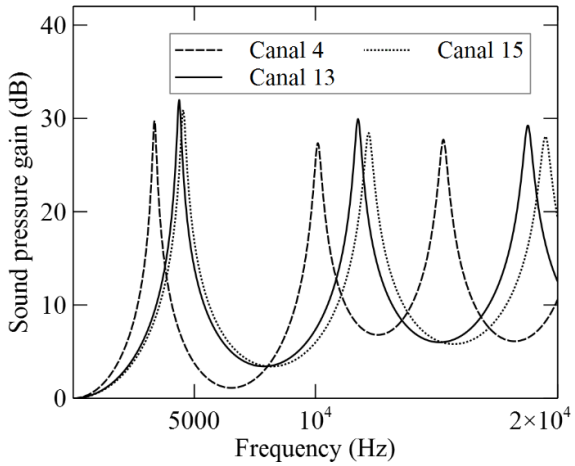


Fig. 17: Gain of the Left Ear Canal with Concha and Eardrum Effect.

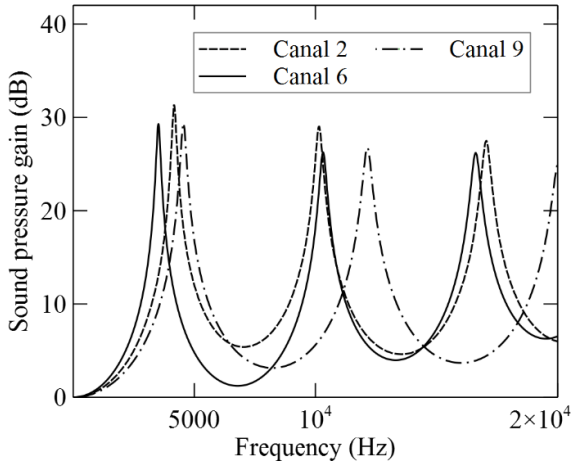


Fig. 18: Gain of the Right Ear Canal with Concha and Eardrum Effect.

8. Conclusion

An acoustic model has been developed using four types of acoustic resonator to better approximate the real shape of the outer ear. This model can be applied to the concha, the ear canal and to the residual ear (Eardrum effect). The proposed model has been validated against results encountered in the literature.

A parametric study shown that the concha has the effect of increasing the value of the resonant frequency when taken into consideration in the modeling. In the other hand, taking into account the real shape of the residual ear acts on the eardrum impedance and decreases the values of resonant frequencies along with the sound pressure gain of the outer ear.

This acoustic model can be used to study diseases in the outer ear by adjusting the resonator parameters.

References

[1] P. W. Alberti, “The anatomy and physiology of the ear and hearing,” Univ. Toronto, Toronto, Canada, Tech. Rep, (2006).

[2] J. K. Moore and F. H. J. Linthicum, “Myelination of the human auditory nerve: different time courses for Schwann cell and glial myelin”, *Annals of Otology, 4hinology and Laryngology*.110 (7),

(2001), pp. 655-661. Available online: 10.1177/000348940111000711
[3] J. A. Johnson, J. Xu, R M. Cox, "Impact of Hearing Aid Technology on Outcomes in Daily Life III: Localization," *Ear Hear*.38 (6), (2017), pp.746-759. Available online: 10.1097/AUD.0000000000000473
[4] R. Z. Gan, B. Feng, and Q. Sun, "Three-dimensional finite element modelling of human ear sound transmission," *Annals of Biomedical Engineering*. 32(6), (2004), pp.847-859. https://doi.org/10.1023/B:ABME.0000030260.22737.53.
[5] C. Giguere and P. C. Woodland. "A computational model of the auditory periphery for speech and hearing research. I. Ascending path," *J. Acoustic. Soc. Am*. 95(1). (1993), pp. 343-349. https://doi.org/10.1121/1.408367.
[6] M. Hiipakka, M. Tikander, and M. Karjalainen, (2010). "Modeling of external ear acoustics for insert headphones usage," *J. Audio Eng. Soc*. 58(4), pp. 269-281.
[7] Open Stax College (2015, May), *Anatomy & Physiology*. OpenStax CNX
[8] R. L. Goode, M. Killion, K. Nakamura, and S. Nishihara, "New knowledge about the function of the human middle ear: Development of an improved analog model," *IEEE Transactions on Biomedical Engineering.* 15(2), (1994), pp. 145-154.
[9] H. Hudde and A. Engel, "Measuring and modeling basic properties of the human middle ear and ear canal. Part II: Ear canal, middle ear cavities, eardrum, and ossicles," *Acta Acustica united with Acustica*, 84(5), (1998), pp. 894–913.
[10] T. Thejane, F. V. Nelwamondo, T. C. Malumedzha, and T. Marwala (2011). "Otoacoustic emissions: A review on existing human auditory system modelling approaches," in *Proceedings of the 22nd IASTED International Conference on Modelling and Simulation* (MS 2011), Calgary, Canada, (2011). Available: https://doi.org/10.2316/P.2011.735-096.
[11] T. Thejane, F. V. Nelwamondo, J. E. Smit, and T. Marwala (2012). "Influence of the Auditory Canal Number of Segments and Radius Variation on the Outer Ear Frequency Response," in *Proceedings of the IEEE-EMBS International Conference on Biomedical and Health Informatics* (BHI 2012), Hong Kong and Shenzhen, China, Jan 2-7, (2012). https://doi.org/10.1109/BHI.2012.6211595.
[12] L. Zheng, Y. T. Zhang, F. S. Yang, and D. T.Ye, "Synthesis and decomposition of transient-evoked otoacoustic emissions based on an active auditory model," *IEEE Transactions on Biomedical Engineering*, 46, (1999), pp. 1098-1106. https://doi.org/10.1109/10.784141.
[13] G. Volandri, C. Carmignani, F. D. Puccio and P. Forte, "Finite Element Formulations Applied to Outer Ear Modeling," *Journal of Mechanical Engineering*, 60(5), (2014), pp. 363-372. Available online: 10.5545/sv-jme.2014.1837
[14] H. Deng and J. Yang, "Modeling and estimating acoustic transfer functions of external ears with or without headphones," *The Journal of the Acoustical Society of America*, 138(2), (2015), pp. 664-707. Available online: https://doi.org/10.1121/1.4926560.
[15] Handbook of Sensory Physiology, S. *EAG*., New York, (1974), pp. 455-490.
[16] A. G. Webster, ''Acoustical impedance, and the theory of horns and of the phonograph,'' *Proc. Natl. Acad. Sci.* U.S.A. 5, (1919), pp. 275–282. https://doi.org/10.1073/pnas.5.7.275.
[17] M. L. Munjal, "Acoustics of Ducts and Mufflers with Application to Exhaust and Ventilation System Design". *Wiley*, New York, (1987).
[18] P. M. Morse, "Vibration and Sound", *McGraw-Hill*, New york, (1948).
[19] ISO 10534-2, Acoustics—Determination of Sound Absorption Coefficient and Impedance in Impedance Tubes–Part 2: Transfer Function Method, *International Organization for Standardization*, Geneva, Switzerland, (1998).
[20] B.B. Bauer, "On the equivalent circuit of a plane wave confronting an acoustical device", *J. Acoust. Soc. Am.* 42, (1967), pp.1095-1097 https://doi.org/10.1121/1.1910695.
[21] M.R. Stinson and B.W. Lawton, "Specification of the geometry of the human ear canal for the prediction of sound-pressure level distribution," *The Journal of the Acoustical Society of America*, 85(6), (1989), pp. 2492-2503. https://doi.org/10.1121/1.397744.
[22] M. R. Stinson, G. A. Daigle, "An eardrum impedance simulator for use with physical replicas of the human ear canal*," The Journal of the Acoustical Society of America*, 127(3), (2010), pp.1868. Available online: 10.1121/1.3384499.